Numerical Simulation of the Electrical Double Layer Development: Physicochemical Model at the Solid and Dielectric Liquid Interface for Laminar Flow Electrification Phenomenon

Mohamed EL-Adawy, Thierry Paillat, Gérard Touchard
Electro-Fluid Dynamics Group, Institut P' UPR 3346 CNRS
University de Poitiers, ENSMA
86962 Futuroscope Chasseneuil, France

and **Juan Martin Cabaleiro**
CONICET, Laboratorio de Fluidodinámica, Departamento de Ingenieria Mecánica
Faculty of Engineering, University of Buenos Aires, Argentina

ABSTRACT

At the solid-liquid interface, a charge zone called the Electrical Double Layer (EDL) appears. It is constituted of two zones of opposite sign, one in the solid and another one in the liquid. When a liquid flows through a pipe, there is a disturbance of the EDL and an axial streaming current is generated. This current is due to the convection of the charges coming from the electrical double layer. In this paper, we present a numerical simulation of the EDL development process in the case of a liquid containing additives or impurities which are partially dissociated into positive and negative ones. We treat the case of laminar flow and an interfacial reaction whose conversion is small compared to the concentration of positive and negative ions in the bulk solution. The boundary conditions are deduced from the kinetics of the wall surface reactions with additives. However, in this paper, the formation of the EDL at the solid-liquid interface is investigated without any flow (static case). Thus, the rate of the wall reaction and the resulting charge concentration in the liquid can be studied. Then, once the equilibrium of physicochemical reaction is reached, convection is forced and the EDL dynamic behavior has been studied (dynamic case). The physicochemical reaction at the solid-liquid interface, the evolution of the space charge density in terms of both the axial coordinates and flow velocity, and the equations of conservation of charge of the liquid species have been implemented to a developed version of "Electricité de France" finite volume CFD tool Code_Saturne®, which is designed to solve the Navier-Stokes equations. Finally, the simulation results of the dynamic behavior at different flow rates are compared with the experimental results.

Index Terms — **Electrical double layer, Flow electrification, Physicochemical corrosion model, Streaming current**

1 INTRODUCTION

FLOW electrification has been extensively studied, since over 50 years ago, due to its economical and theoretical interest. This phenomenon, first occurring in the petroleum industry, appeared to be the responsible for major incidents in oil-cooled power apparatus such as transformers, in which oil flow is used to cool the system, and remains an important problem faced by electric power industry [1-5]. Concerning analysis of the phenomenon, its evolution in terms of flow and pipe geometry is now rather well understood and established. However one of the most important parameters, which control the diffuse layer development in the liquid and consequently the space charge density, is the physicochemical process at the origin of the phenomenon. To date, this physicochemical process is still under investigation [5-9].

This phenomenon, occurring in the oil-cooled power apparatus, needs further study to obtain a reliable design of such apparatus particularly with regard to the charge separation process occurring at the solid-liquid interface. Convection of liquid creates a streaming current and leads to a continuous charge separation

Manuscript received on 27 October 2010, in final form 14 April 2011.

process at the interface. When the solid is an insulator, leakage impedances limit the accumulation of these charges at the wall. This leads to potential buildup and hence discharges on the surface of the solid material. Finally it may cause major discharge damage as in the case of large oil-cooled power transformers.

From the theoretical point of view, many papers have been published which deal with the mathematical description of the Electrical Double Layer (EDL) [6-8]. These papers describe the distribution of the potential or of the space charge density in the liquid. They are always based on one parameter, which depends only on the physicochemical proprieties of both the solid and the liquid. In most cases, this parameter is the zeta potential (ζ) or the Helmholtz potential (ψ_0). In other cases, it is the space charge density on the wall (ρ_{wd}) for a fully-developed EDL [9]. Also, the diffuse layer thickness (δ_0) and the EDL development time (τ) should be considered due to their effect on the EDL.

One of the most important parameters, the physicochemical reaction at the pipe wall-liquid interface which induces the flow electrification remains very difficult to quantify. When a liquid is in contact with a solid surface, a physicochemical reaction occurs at the solid-liquid interface, leading to the formation of an EDL. The process of flow electrification is caused by the axial convection of the diffuse liquid part of the EDL appearing at the solid-liquid interface. Thus, the rate of the wall reaction and the resulting charge concentration in the liquid may control the flow electrification.

Nevertheless, there are benefits to be derived from computational models, particularly when they are calibrated with empirical results. Although precision is unattainable, much information about the trends and relative performances of various systems and operating condition may be obtained. A computational model may provide such information without the expense and effort required for the implementation of a physical model. Furthermore, some parameters of the physical model, such as the spatial development of the charge profile, may not be measurable to the desired resolution without significantly disturbing the system.

The purpose of this paper is to introduce a physicochemical model, analogous to the corrosion model [5], and a numerical simulation of the EDL development process in the case of a solid wall and a liquid containing additives or impurities which are partially dissociated into positive and negative ions. We treat the case of laminar flow and an interfacial reaction [10-14] whose conversion is small compared to the concentration of positive and negative ions in the bulk solution. However, the formation of the EDL at the solid-liquid interface is investigated without any flow to study the effect of physicochemical reaction on the space charge density especially when changing the concentration of liquid impurities. Then, once the equilibrium of the physicochemical reaction is reached, convection is forced and the EDL dynamic behavior has been studied.

2 A PHYSICOCHEMICAL MODEL

As soon as the liquid is in contact with the solid surface, the complex solid-liquid initially neutral becomes polarized under physicochemical reactions occurring at the interface. Such reactions generate a specific value of the streaming current depending on the type of the solid material and the chemical composition of the liquid, such as transformer oil, which is difficult to be characterized.

Furthermore, even in a highly purified state, the hydrocarbon liquid oil can contain impurities that can undergo chemical reactions and affect the charge generated by flow electrification. Since these impurities are usually present in trace amounts, their composition tends to be unknown [15]. Also, additives may be used intentionally, e.g. to reduce the electric resistivity of the liquid or to significantly modify the EDL.

The physicochemical corroding model [5] has been developed in the case of a conductive solid in contact with a dielectric liquid containing additives or impurities partially dissociated into positive and negative ions. In our model, we assume a mechanism analogue to this model for the case of dielectric solid. Hence, the impurity or additive A_LB_L is weakly dissociated in the liquid. Thus we have the following equation [5]:

$$A_LB_L \underset{k_{r1}}{\overset{k_{d1}}{\rightleftharpoons}} A_L^+ + B_L^- \tag{1}$$

where k_{d1} and k_{r1} are the kinetic constants of the dissociation and recombination reactions, respectively.

As a result of the chemical reactions, the concentrations of the species will change with time. The equation that describe these chemical kinetics for uniform concentrations are

$$\begin{aligned} \frac{d[A_L^+]}{dt} &= \frac{d[B_L^-]}{dt} = -\frac{d[A_LB_L]}{dt} \\ &= k_{d1}[A_LB_L] - k_{r1}[A_L^+][B_L^-] \end{aligned} \tag{2}$$

where the $[X]$ symbols denote the molar concentration or number density of species X. The first term on the right side of equation (2) gives the rate of generation of ions (A_L^+ and B_L^-) from the dissociating neutral molecule A_LB_L, while the second term gives the rate of recombination of the ions to form the neutral molecule. While this description of chemical kinetics is valid only for a fully mixed system, most systems have spatial variations.

A general formulation for the kinetics can be derived by balancing the time rate of change of the concentration of each species in a differential volume to the flux through the surface enclosing the volume and any chemical reactions inside the volume. This conservation equation can be written as [16]:

$$\frac{\partial n_i}{\partial t} + \vec{\nabla} \cdot \vec{\Gamma}_i = G_i - R_i \tag{3}$$

where the subscript i denotes the i^{th} species, n_i is the number density, $\vec{\Gamma}_i$ is the flux, and G_i and R_i represent the generation

and recombination due to the chemical reaction. This is equivalent to equation (2) if the convective derivative is taken.

It is also assumed that the fluid is an incompressible liquid with the flow imposed by an external mechanical system. This implies that any electrical forces on the charged fluid are negligibly small so that the fluid mechanics are decoupled from the electrical laws.

In order for an electrical double layer to be developed between the fluid phase and solid one, a chemical dissociation reaction must occur at the interface or a charged species must accumulate at the interface. Both of these processes can be described as heterogeneous reactions because they occur between different phases.

The basic steps for heterogeneous reactions are: the dissociation reaction at the solid interface, the transport of the reactants from the solid interface to the fluid, the reaction (recombination and dissociation) in the liquid region and the transport of reactants (products) away from the surface of reaction. The transport mechanism to and from the surface is usually taken to be diffusion, but fluid convection and the migration of charged species also serve as transport mechanisms [15]. These surface reactions lead to the boundary conditions on the flux of species from and to the interface.

When an initially electrically neutral liquid comes in contact with a solid surface, a physicochemical reaction starts at the solid-liquid interface. This reaction depends on the nature of the solid and the liquid impurities.

Also, it is assumed that the solid surface is partly or totally composed of molecules C_sD_s and undergoes the following reaction in presence of the liquid

$$C_sD_s \underset{k_{r2}}{\overset{k_{d2}}{\rightleftarrows}} C_s^+ + D_s^- \tag{4}$$

where k_{d2} and k_{r2} are the kinetic constants of the wall dissociation and recombination reactions, respectively. Then when the cations C_s^+ are in contact with the anions of the liquid B_L^-, a surface reaction can occur in the liquid region as follows:

$$C_s^+ + B_L^- \underset{krp}{\overset{k_{fp}}{\rightleftarrows}} C_sB_L \tag{5}$$

where k_{fp} and k_{rp} are the kinetic constants for the forward and reverse reactions, respectively. Thus, two kinds of neutral impurities, A_LB_L and C_SB_L, now exist in the liquid.

Reactions (1), (4) and (5) are equivalent to a positive current at the solid-liquid interface, and they lead to an accumulation of positive ions in the liquid, while the negative ones react on the solid. The net reaction stops when the concentration of anions B_L^- and cations C_s^+ are such that the reaction (5) is in equilibrium. From the electrical point of view, this means that the space charge density in the liquid near the wall reaches a constant value. In the following section, we investigate this scenario.

3 CHARGE-TRANSPORT MECHANISMS

In modeling charge-re-distribution processes, it is assumed that transport of charges occurs by three different mechanisms: migration, convection and diffusion.

The net current density $\vec{J}$ is the sum of these three components. After the initial charge distribution has been determined, the potential distribution had to be calculated. Assuming that the system is electroquasistatic, the electric field can be determined from the electric scalar potential φ. Thus, the basic driving equation was Poisson's equation.

The flux term gives the transport of each species through the fluid. It is generally stipulated by a constitutive law that accounts for diffusion, convection and drift if the species is charged. The net flux densities of all species in the oil zone (medium 1) can be expressed as:

$$\begin{aligned}
\overrightarrow{\Gamma_L^+} &= -D_1^+\vec{\nabla}n_L^+ - n_L^+\frac{e_0.z_P.D_1^+}{kT}\vec{\nabla}\varphi + n_L^+\vec{u}\\
\overrightarrow{\Gamma_L^-} &= -D_1^-\vec{\nabla}n_L^- + n_L^-\frac{e_0.z_N.D_1^-}{kT}\vec{\nabla}\varphi + n_L^-\vec{u}\\
\overrightarrow{\Gamma_L^{neut}} &= -D_1^{neut}\vec{\nabla}n_L^{neut} + n_L^{neut}\vec{u}\\
\overrightarrow{\Gamma_S^+} &= -D_1^+\vec{\nabla}n_S^+ - n_S^+\frac{e_0.z_P.D_1^+}{kT}\vec{\nabla}\varphi + n_S^+\vec{u}\\
\overrightarrow{\Gamma_{SL}^{neut}} &= -D_1^{neut}\vec{\nabla}n_{SL}^{neut} + n_{SL}^{neut}\vec{u}
\end{aligned} \tag{6}$$

and the net flux densities in the solid interface region (medium 2) are as follows:

$$\begin{aligned}
\overrightarrow{\Gamma_S^+} &= -D_2^+\vec{\nabla}n_S^+ - n_S^+\frac{e_0.z_P.D_2^+}{kT}\vec{\nabla}\varphi\\
\overrightarrow{\Gamma_S^-} &= -D_2^-\vec{\nabla}n_S^- + n_S^-\frac{e_0.z_N.D_2^-}{kT}\vec{\nabla}\varphi\\
\overrightarrow{\Gamma_S^{neut}} &= -D_2^{neut}\vec{\nabla}n_S^{neut}
\end{aligned} \tag{7}$$

Thus, the conservation equations of each species in the oil region can be written as follows:

$$\begin{aligned}
\frac{\partial n_L^+}{\partial t} + \vec{\nabla}\cdot\overrightarrow{\Gamma_L^+} &= k_{d1}n_L^{neut} - k_{r1}n_L^+n_L^-\\
\frac{\partial n_L^-}{\partial t} + \vec{\nabla}\cdot\overrightarrow{\Gamma_L^-} &= k_{d1}n_L^{neut} - k_{r1}n_L^+n_L^- + k_{rp}n_{SL}^{neut} - k_{fp}n_S^+n_L^-\\
\frac{\partial n_L^{neut}}{\partial t} + \vec{\nabla}\cdot\overrightarrow{\Gamma_L^{neut}} &= k_{r1}n_L^+n_L^- - k_{d1}n_L^{neut}\\
\frac{\partial n_S^+}{\partial t} + \vec{\nabla}\cdot\overrightarrow{\Gamma_S^+} &= k_{rp}n_{SL}^{neut} - k_{fp}n_S^+n_L^-\\
\frac{\partial n_{SL}^{neut}}{\partial t} + \vec{\nabla}\cdot\overrightarrow{\Gamma_{SL}^{neut}} &= k_{fp}n_S^+n_L^- - k_{rp}n_{SL}^{neut}
\end{aligned} \tag{8}$$

and in the solid region, these equations are as follow:

$$\begin{aligned}
&\frac{\partial n_S^+}{\partial t} + \vec{\nabla}\cdot\overrightarrow{\Gamma_S^+} = k_{d2} n_S^{neut} - k_{r2} n_S^+ n_S^- \\
&\frac{\partial n_S^-}{\partial t} + \vec{\nabla}\cdot\overrightarrow{\Gamma_S^-} = k_{d2} n_S^{neut} - k_{r2} n_S^+ n_S^- \\
&\frac{\partial n_S^{neut}}{\partial t} + \vec{\nabla}\cdot\overrightarrow{\Gamma_S^{neut}} = k_{r2} n_S^+ n_S^- - k_{d2} n_S^{neut}
\end{aligned} \tag{9}$$

The above equations are coupled to the Poisson's equation in each corresponding region, in the liquid:

$$\varepsilon_1 \nabla^2 \varphi = -e_0 \left(z_P n_L^+ - z_N n_L^- + z_P n_S^+ \right) \tag{10}$$

and in the solid region

$$\varepsilon_2 \nabla^2 \varphi = -e_0 \left(z_P n_S^+ - z_N n_S^- \right) \tag{11}$$

where:

$\overrightarrow{\Gamma_{L,S}^{+,-}}$	Ionic flux density vector ($m^2.s^{-1}$)
$\overrightarrow{\Gamma_{L,S}^{neut}}$	Neutral flux density vector ($m^2.s^{-1}$)
$D_{1,2}^{+,-,neut}$	Positive, negative or neutral diffusion coefficient in the corresponding medium ($m^2.s^{-1}$)
$n_{L,S}^{+,-,neut}$	Positive, negative or neutral species number concentration in the corresponding medium (m^{-3})
e_0	Charge of electron (1.6022×10^{-19} C)
$z_{P,N}$	Positive/negative ions valence, taken as 1
k	Boltzmann's constant (1.38×10^{-23} J/K)
T	Absolute temperature (K)
ε_i	Dielectric permittivity of the medium
φ	Electric scalar potential (V)
$\vec{u}$	Velocity vector ($m.s^{-1}$)

Finally, in the liquid region, due to the convective transport of the species which are present in the medium, the previous equations are coupled to Navier-Stokes equations (incompressible Newtonian fluid of constant mean velocity):

$$\begin{aligned}
\rho_m \frac{D\vec{u}}{Dt} = &-\vec{\nabla}P + \rho_m \vec{g} + \eta \Delta \vec{u} \\
&- e_0 \left(z_P n_L^+ - z_N n_L^- + z_P n_S^+ \right) \vec{\nabla}\varphi
\end{aligned} \tag{12}$$

where ρ_m is the mass density, P is the pressure and η is the dynamic viscosity of the liquid.

The previous system of equations has been implemented to a developed version of "Electricité de France (EDF)" finite volume CFD tool Code_Saturne® [17-19], which is designed to solve the Navier-Stokes equations in the cases of 2D, 2D axisymmetric or 3D flows.

In order to separate between the chemical phenomenon and the influence of liquid convection, the simulation is undertaken in two phases:

1) Static development of the EDL: starting from uniform initial conditions of all species, the previous dissociation and recombination reactions are allowed to start and the simulation is continued until the electric current through the interface becomes negligible or the space charge density at the interface becomes nearly constant.
2) Once the static equilibrium has been reached, a Posieuille flow is imposed at the entry and the effect of convection is studied.

This simulation procedure enables to relay the model to each of its components (influence of chemical regime and convection). Furthermore, it reflects the reality of our experiences.

4 THE INITIAL GUESS ESTIMATION

In order to compare the model to the experimental data, the initial concentration of species and the chemical reaction rates should be estimated. One of the most difficult is to find and define the parameters that are used as initial conditions for the simulation. These parameters include the ionic species, the ionic diffusivity and the chemical reaction rates. Empirically, the ion mobility (m^2/Vs) in hydrocarbon liquids is related to the dynamic viscosity η (kg/ms) by Walden's rule as [15]

$$\mu_L \eta \approx 2\times10^{-11} \qquad C/m \tag{13}$$

where μ_L is the ionic mobility of liquid species.

Tobazéon [20] has introduced a simplified procedure for the calculation of the initial concentration of oil species and the constants of the reaction rates with the help of the physical constants of the liquid under test. Details of the oil characteristics and operational parameters are given in Table 1. From these constants, we can calculate the initial concentrations of all species in the liquid region as has been observed in [21]. The recombination coefficient is related to the oil's permittivity and the ions mobility by the Langevin relation [20]:

$$k_{r1} = \frac{e_0}{\varepsilon_1} \left(\mu_L^+ + \mu_L^- \right) \tag{14}$$

The diffusivity and mobility are related through the Einstein's relation

$$\frac{D_1^{+,-}}{\mu_L^{+,-}} = \frac{kT}{e_0 \left| z_{P,N} \right|} \tag{15}$$

The diffusion flux is based on the Fick's law and the assumption that the species are present in trace quantities so that each species diffuses independently [22]. Also, the diffusion coefficient of the oil neutral species is given by [20]:

Table 1. Physical constants for the transformer oil under test at 20 °C.

Symbol	Quantity	Value
σ_0	Oil bulk conductivity	0.5×10^{-13} S/m
ε_1	Transformer oil permittivity	$2.2\varepsilon_0$
η	Dynamic viscosity	0.0146 kg/(m.s)
ρ_m	Oil mass density	836.9 kg/m^3
μ_L^+	Mobility of oil positive ions	10^{-10} m^2/(V.s)
μ_L^-	Mobility of oil negative ions	10^{-10} m^2/(V.s)
z	Ions Valence	1
$q=ze_0$	Ions charge	1.6×10^{-19} C
D_1^+	Diffusion coefficient of oil positive ions	2.5×10^{-12} m^2/s
D_1^-	Diffusion coefficient of oil negative ions	2.5×10^{-12} m^2/s
δ_0	Debye length	31.4×10^{-6} m

$$D_1^{neut} = D_0 = \frac{2D_1^+ D_1^-}{D_1^+ + D_1^-} \tag{16}$$

At the beginning of the simulation, the space charge density is zero throughout the entire volume, the initial positive and negative ion concentrations are equal. Also, the chemical species have the following form at the equilibrium condition:

$$k_{d1} n_{L0}^{neut} = k_{r1} n_{L0}^+ n_{L0}^- \tag{17}$$

where n_{L0}^{neut}, n_{L0}^+ and n_{L0}^- are the initial concentration of neutral species, positive and negative ions in the liquid, respectively. Combining (17) and (14), we obtain:

$$k_{d1} = \frac{e_0}{\varepsilon_1}(\mu_L^+ + \mu_L^-)\frac{{n_{L0}^+}^2}{n_{L0}^{neut}} \tag{18}$$

Defining p as an ionization factor which is related to the ionization fraction θ by:

$$p = \frac{\theta}{1-\theta} = \frac{n_{L0}^+}{n_{L0}^{neut}} \tag{19}$$

Thus, for a known initial concentration, the dissociation reaction rate can be estimated by:

$$k_{d1} = \frac{e_0}{\varepsilon_1}(\mu_L^+ + \mu_L^-) n_{L0}^+ p \tag{20}$$

An order of magnitude for the initial concentration can be estimated from the liquid's bulk conductivity as shown [20]:

$$\sigma_0 = e_0 n_{L0}^+ (\mu_L^+ + \mu_L^-) \tag{21}$$

For an ionized fraction of 0.1 [21], (which is quite high), the initial concentrations and chemical reaction rates for the liquid under test, which is mentioned in Table 1, can be estimated. These values are summarized in Table 2.

In our model, we assume that the concentration of the neutral species $C_S D_S$ is so large that there is always enough $C_S D_S$ for the dissociation reaction (4). However, with this very high molecular concentration, there is no impact on the simulation results when keeping this value as very high as compared to the other concentrations.

The constants k_{d2} and k_{r2} have been determined to ensure that the concentration of positive ions in the solid, at the equilibrium, is in the same order of magnitude as that for the liquid. So, this value is assumed to be 10^{15} ions/m^3. At the equilibrium of the reaction (4), we have the following:

$$k_{d2} n_{S0}^{neut} = k_{r2} n_{Seq}^+ n_{Seq}^- \tag{22}$$

where n_{Seq}^+ and n_{Seq}^- referring to the concentration of positive and negative ions, respectively, at the equilibrium conditions or when the electrical double layer is fully developed.

Inside the liquid, the Stern model [5] distinguishes two different regions: the compact layer so close to the wall that its electrical charges are not affected by the liquid flow, and the diffuse layer for which the space charge density ρ decreases when one moves away from the wall. At the wall, there is a maximum value of space charge which is known as the fully developed space charge density ρ_{wd}. So the classical form for the wall current is the following [2]:

$$i_w = K(\rho_{wd} - \rho_w) \tag{23}$$

i_w being the wall current density produced by the reaction at the interface, while the coefficient K is related to the intensity of the physicochemical reactions (in the classical model it is considered to be only dependent on the liquid-solid couple).

Starting from the principle of charge conservation with the assumption of weak space charge density, one can obtain the following expression for the coefficient K as in [2, 23]:

$$K = \frac{V}{A} k_{fp} \frac{n_{Seq}^+ n_{L0}^-}{2(n_{L0}^- - n_{Leq}^-)} \tag{24}$$

Here V is the volume of the liquid in contact with the wall of surface area A. The ratio between the volume and the surface of contact can be considered to equal the Debye length δ_0. n_{Leq}^- is the concentration of liquid negative ions for a fully developed double layer, which can be neglected when it is compared to the initial liquid concentrations.

The recombination rate for the solid-liquid reaction can be determined as follow:

$$k_{fp} \approx \frac{A}{V}\frac{2K}{n_{Seq}^+} = \frac{1}{\delta_0}\frac{2K}{n_{Seq}^+} \tag{25}$$

Table 2. Initial values and chemical reaction rates.

Symbol	Quantity	Value
$n_{L0}^{+,-}$	Initial concentration for positive and negative ions in the liquid	1.56×10^{15} ions/m^3
n_{L0}^{neut}	Initial concentration of neutral molecules in the oil	1.40×10^{16} molec./m^3
$n_{S0}^{+,-}$	Initial concentration for positive and negative ions in the solid	0
n_{S0}^{neut}	Initial concentration of neutral molecules in the solid region	10^{27} molec./m^3
K	Physicochemical reaction constant	2.0×10^{-6} m.s^{-1}
k_{d1}	Dissociation rate in the oil	2.85×10^{-4} s^{-1}
k_{r1}	Recombination rate in the oil	1.65×10^{-18} m^3.s^{-1}
k_{d2}	Dissociation rate in the solid	1×10^{-14} s^{-1}
k_{r2}	Recombination rate in the solid	2.81×10^{-19} m^3.s^{-1}
k_{fp}	Recombination rate for the solid-liquid reaction	1.27×10^{-17} m^3.s^{-1}
k_{rp}	Dissociation rate for the solid-liquid reaction	1.27×10^{-4} s^{-1}

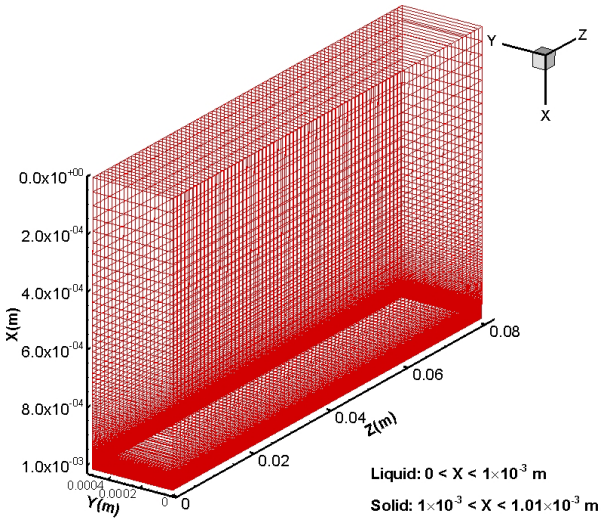

Figure 1. The coordinate system and mesh used for the simulations (darker regions have higher grid densities).

Furthermore, at the equilibrium condition of the solid-liquid reaction, we have following:

$$k_{rp} n_{SLeq}^{neut} = k_{fp} n_{Seq}^{+} n_{Leq}^{-} \tag{26}$$

where n_{SLeq}^{neut} is the concentration of the resulting neutral molecules from the solid-liquid reaction for a fully developed double layer. As this concentration increases when decreasing the negative ion concentration of the liquid, the ratio between these concentrations is unknown. Several values have been tested and have to be adjusted. The present results are corresponding to a ratio of 1000 between the concentrations of resulted neutral molecule and the liquid negative ions.

Thus, for a physicochemical reaction constant K= 2×10^{-6} m/s [1, 2, 10, 21], Table 2 summarizes the initial concentrations and the reaction rates for the couple, solid-liquid, under test.

5 THE IMPLEMENTATION OF THE SIMULATION

5.1 THE SYSTEM GEOMETRY

The considered geometry, which is used for this simulation, is based on the rectangular configuration sensor prototype of our experimental facility which is used to obtain the experimental results. A precise description of this facility and the sensor is described in details in [24, 25]. In this facility, the streaming current is experimentally produced by the oil flowing through the rectangular channel (3 mm ×30 mm cross-section and 300 mm in length) as a function of oil mean flow velocity and also as a function of time interval (at rest) between two consecutive runs [1, 10, 26]. The general geometry covered in the scope of the simulations performed here is depicted in Figure 1.

If the walls of the channel are sufficiently separated, the charge distribution near one wall will be unaffected by the opposite wall, so only one wall and leading edge need to be analysed. Furthermore, to reduce the time of calculation, only 80 mm in length has been considered in this simulation. We considered a rectangular geometry in which the thickness is large compared to δ_0. In this condition, the problem could be considered to be a planar interface. The system was assumed to be invariant in the Y direction. The Z axis was horizontal, parallel to the mean flow, with zero at the leading edge of the channel. The X axis was aligned perpendicular to the channel walls with zero at the channel centre. The grid used for these calculations was a rectangular mesh, so that derivatives could be calculated along lines of constant X and constant Z.

For a good resolution near the wall, the step size in that region must be less than that the Debye length [27], so a variable step size was used to reduce the memory requirement. Hereby, we have 9600 cells (120×1×80) in the liquid region and 1600 cells (20×1×80) in the solid one. The liquid exists between 0<X<1 mm with a minimum mesh size of 1.1×10^{-7} m and 5×10^{-5} m of maximum size. With this non-uniform mesh, there are 50 cells in the Debye length δ_0 and 75 in a distance of $3\delta_0$.

5.2 BOUNDARY CONDITIONS

In addition to the equations describing the dynamics of the charged species in the bulk of the fluid, the boundary conditions are critically important. For the model described here, spatial boundary conditions were needed for the wall, upstream border and the downstream border.

All the present results in this paper are two dimensional, so that boundary conditions of symmetry (Neumann conditions) are defined in the Y direction. In the X direction, boundary conditions of symmetry are also defined at X= 0 (half of the channel), based on the assumption that there is symmetry about the spacers.

At the leading edge of the region of computation, it was assumed that the incoming fluid was uncharged, so Dirichlet conditions were also used here, with a fixed value of zero charge density.

The trailing edge of the region of computation was also defined as a Neumann condition, which assumed that the charge profile in the fluid was fully developed [27].

A wall boundary condition (Neumann conditions) [21] has been defined at X= 1.01 mm for all the scalar variables. For the electric potential, a Dirichlet boundary condition has been defined which enables us to fix the value of the potential at the border of the downstream region (*e.g.*, φ= 0 V).

Finally, for the static case only, in the Z direction, symmetrical boundary conditions have been imposed based on the assumption that there is symmetry about the spacers for a no fluid flow case.

An example case is now presented based on both the physical constants which are summarized in Table I and the estimated constants of Table 2.

6 TIME EVOLUTION OF THE STATIC SPACE CHARGE DENSITY

Before fluid flow in introduced, it is useful to explore some of the implications of this chemical reaction based static space charge density. In the absence of fluid motion, the system will reach an equilibrium state depending upon the chemical kinetics of the ionizable impurities and the electrical forces acting upon these species.

Figure 2 shows the concentration of all species at the static equilibrium state. We have observed that, the positive ions of the solid interface were quickly moved to the liquid and reacted with the negative ions of the liquid to create the neutral species n_{SL}. The concentration of liquid negative ions near the interface was almost zero after 150 s which was corresponding to a very low charge density at this point. This lack of negative ions in the liquid produced an imbalance in the dissociation of impurities in the oil. As a result, the oil neutral molecules dissociated to remedy this imbalance, creating new positive and negative ions; the latter reacted instantly, and so on, until the static equilibrium.

Hereby, these chemical reactions are corresponding to an accumulation of positive ions in the liquid and negative at the solid surface as shown from Figure 2. The increase of positive ions in the solid produces a diffusive flux of these species

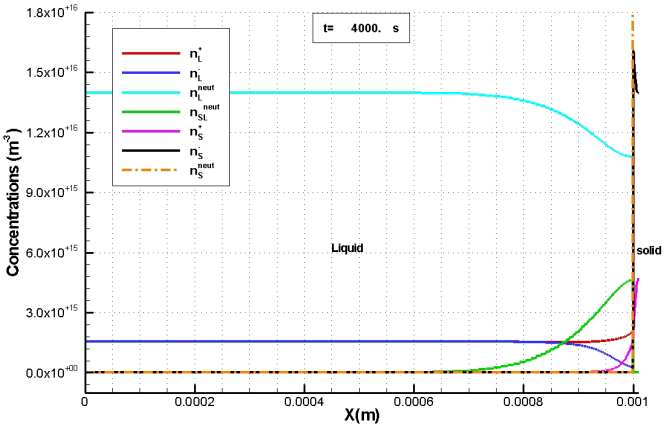

Figure 2. Concentration of all species at static equilibrium.

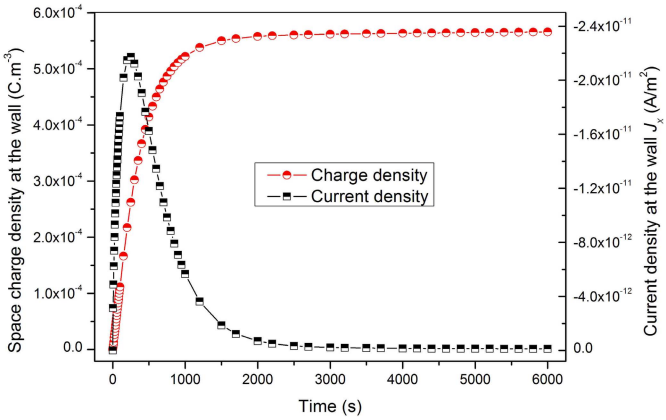

Figure 3. Evolution of both the space charge density and the current density at wall, in the liquid region, until static equilibrium is reached.

towards to the liquid, which increases both the space charge density and the electric field at the interface.

Figure 3 shows the evolution of both the static space charge density at the interface and the current density near the wall, all in the liquid region. This current density can be calculated from the global flux density of the charged species. It is clear that, the static equilibrium is achieved at a time t= 4000 s which is corresponding to either the cancellation of the current density at the interface or a constant space charge density at the interface as shown in Figure 3. In other words, from this instant, the current due to the diffusion of charged species is equal and opposite of the current due to migration. Hence, one can say that the electric field has reached to a highly enough value to prevent the diffusion of charged species.

Figure 4 shows the space charge density at the static equilibrium which is positive in the oil region, and negative in the solid one (as expected). This value is constant in the Z direction which is satisfied with the symmetrical conditions that are imposed in this direction for the static case.

Other profiles are extracted at a fixed plane, (Z= 0.04 m and Y= 0) with varying the X coordinates, to demonstrate the time evolution of the static space charge density as shown in Figure 5. It is clear that, from the first moment when the liquid is put in contact with the solid, a physicochemical reaction occurs at

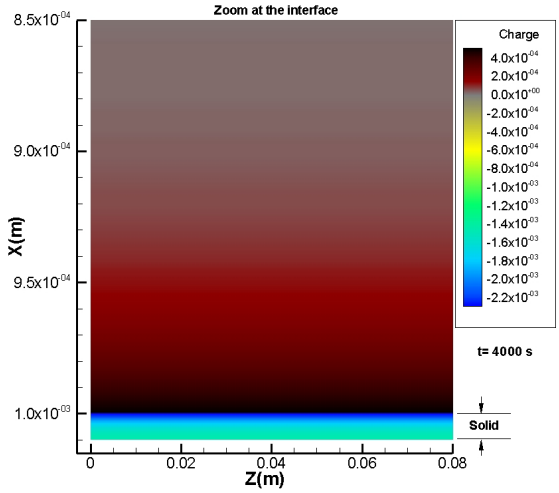

Figure 4. Space charge density (C/m^3) close to the interface. t= 4000 s.

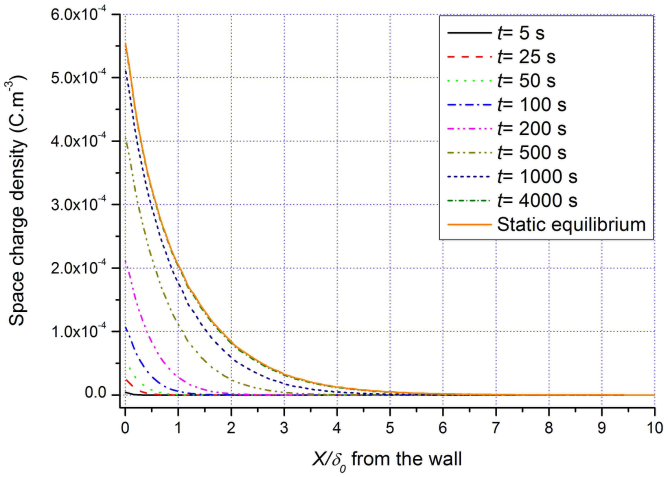

Figure 5. Time evolution of the static space charge density in the liquid region.

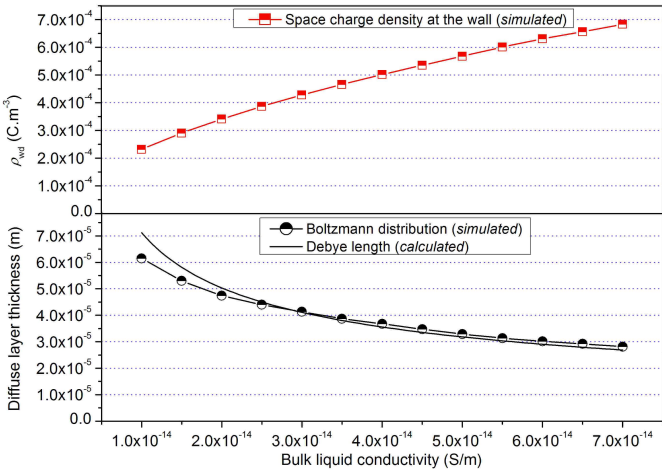

Figure 6. Effect of changing the bulk liquid conductivity on both the space charge density near the wall and the diffuse layer thickness.

their interface leading to a formation of an EDL. Thus, after a time dependent on the initial conditions, the space charge density at the interface reached a maximum value or a fully developed value ρ_{wd} as has been mentioned before.

Previous experiments [28] supposed that the space charge development time in the diffuse layer is much faster than the evolution of the wall space charge density. This means that the relaxation time $\tau_c=\varepsilon/\sigma_0$ is much smaller than the time needed for the development of the diffuse layer at the interface. Under these considerations, the space charge density profile is a quasi-static profile. Thus, it is reasonable to assume that all along the channel axis, the space charge density profile is similar to a fully developed diffuse layer profile.

From these results (Figure 5), one can confirm that it is important to know the space charge density profile for a diffuse layer at rest in the channel (without flow) as has been reported before [2]. Concerning the diffuse layer, its thickness is usually equal to the Debye length given by [9]:

$$\delta_0 = \sqrt{\frac{\varepsilon_1 D_0}{\sigma_0}} \tag{27}$$

Indeed, according to a Boltzmann distribution, 87% of the diffuse layer charges are located between the compact layer and a distance from the wall equal to $2\delta_0$ and 95% for $3\delta_0$ [9]. It is clear that, for the same ε and D_0, the Debye length decreases with the increase of the conductivity (*i.e.* with additive concentrations) which increases the space charge density as has been reported in our experimental facilities [9, 10, 29-31].

In order to simulate this effect, for the same physicochemical reaction coefficient K and for the same liquid diffusion constants, the bulk liquid conductivity has been changed. All the initial concentrations of species and chemical reaction rates are re-calculated according to the simplified procedure which was mentioned before. Figure 6 shows the effect of changing the liquid's bulk conductivity on both the space charge density and the diffuse layer thickness. The upper part of Figure 6 shows the effect of increasing the liquid conductivity on the static space charge density at the wall in the liquid region. One must be very careful when using additives in order to avoid electrostatic hazards. The lower one in Figure 6 shows the effect of liquid conductivity on the Debye length, this length is calculated when the space charge density value is dropped to 13% of its maximum value at the wall and compared with the classical value of the calculated length (27). Therefore, increasing the conductivity will reduce the thickness of the region where the charges are located but at the same time, the amount of charge in the diffuse layer increases dramatically.

7 LAMINAR FLOW ELECTRIFICATION

Obviously a key element of the streaming electrification dynamics is the flow. At the channel entrance, we assume that the space charge density is equal to zero in the entire cross section. As a first approximation, we also assume a fully developed laminar flow at the channel entry to avoid the incidence of any temporal perturbation in the diffuse layer. Thus, the laminar flow velocity is given by the Poiseuille flow equation everywhere:

$$U(x) = \frac{3}{2} U_m \left(1 - \frac{x^2}{a^2}\right) \tag{28}$$

where U_m is the mean flow velocity and a representing the half thickness of the channel.

Once the static equilibrium of the physicochemical reaction is reached, convection is forced to study the EDL dynamic behavior. Figure 7 shows the evolution of the space charge density along the channel under test (Figure 1) for the first five seconds of flow. The scale is reduced to have a closer view at the interface due to the importance of velocity profile which controls the dynamic formation of the EDL. It is clear that, the space charge, which is homogenous along the channel at the beginning, is swept by the fluid flow. It evolves

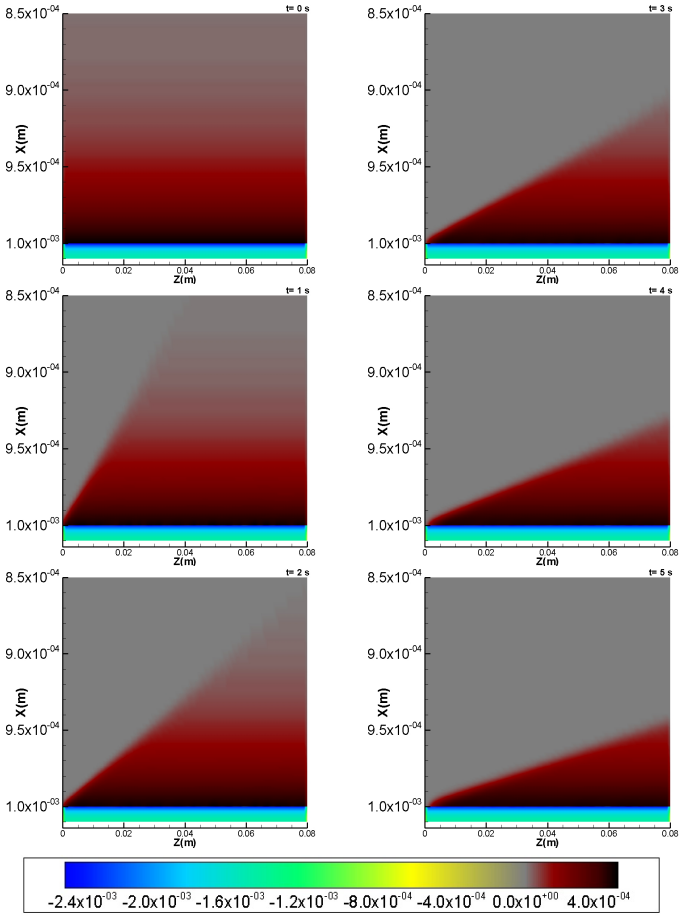

Figure 7. Space charge density (C/m^3) close to the interface. Mean flow velocity 0.1 m/s.

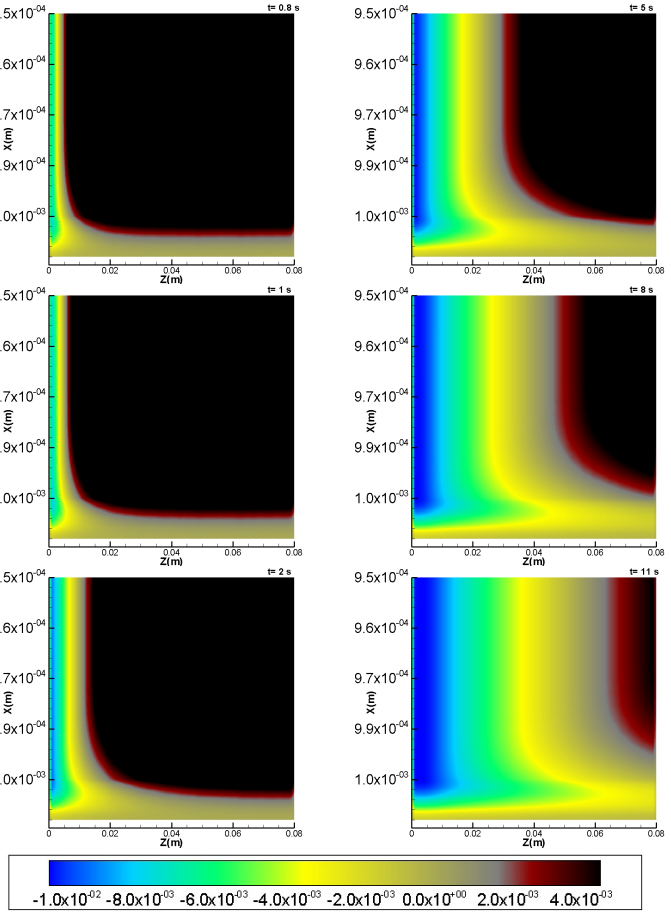

Figure 8. Potential distribution along the channel at different times. Mean flow velocity 0.1 /m/s.

towards a dynamic equilibrium regime where the space charge increases progressively along the channel. Thus, the motion of the fluid redistributes the chemical species. This results in a measurable charge density in the volume of the fluid and a terminal current.

The potential distribution along the channel has been simulated as shown in Figure 8 which gives us an idea about the location of charge accumulation regions. As shown, at the beginning of channel and close to the interface, there is a zone of accumulation of charge. This zone is progressing with time towards the exit of the channel with increasing amplitude.

8 FLOW ELECTRIFICATION CURRENT

The streaming current is simply the integral over the channel area of the convected space charge density, across the trailing boundary, which is given by:

$$I_s = \iint \rho(x,z)\ U(x) ds \tag{29}$$

The evolution of streaming current versus time for four different mean flow velocities is shown in Figure 9. Our experimental facilities [10, 24, 26] show that, the absolute value of the streaming current reaches a maximum, then starts to drop more and less rapidly to constant value. In fact, the peak value represents the convection of a diffuse layer, developed at rest during a time *t*. Once the flow begins, the diffuse layer evolves towards a dynamic equilibrium, which does not depend upon initial conditions.

As shown from this figure, the peak value of the streaming current is proportional to the mean flow velocity as reported before [1-9, 32-42].

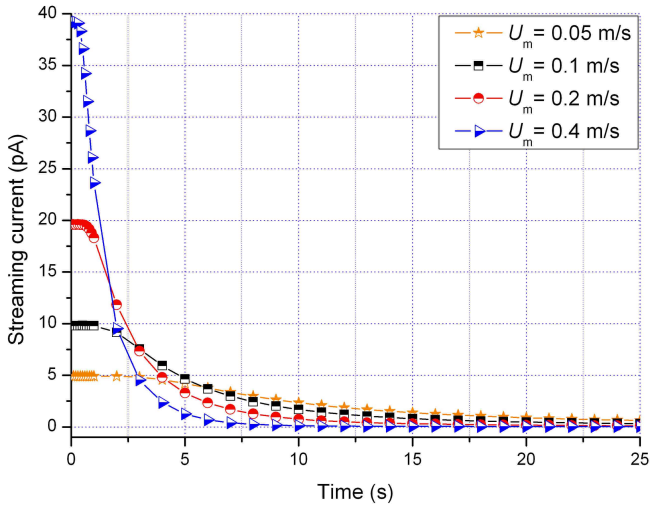

Figure 9. Streaming current (Numerical) as a function of time, for four different mean flow velocities.

Our Experimental facility results [1, 5, 9, 10] show that, the streaming current's peak value is observed at about 5 s after the starting of the pump. In our simulation, this maximum value is reached faster than that. This is probably due to the fact that the velocity profile is imposed instantaneously in the simulation, but the pump takes few seconds for attaining its stationary regime [21]. Also, the filtering associated with the measuring Pico-ammeters contributes in retarding the signal. Nevertheless, there is agreement between the experimental and numerical curves from the dynamics and order of magnitudes points of view.

We have to remark that, however, at t=3 s approximately, the streaming current for the highest velocity (0.4 m.s^{-1}) becomes smaller than that for the lower velocity (0.05 m.s^{-1}). The same trend is observed at t= 5 s between those currents for velocities of 0.1 and 0.2 m.s^{-1} respectively. This particular behavior has not been observed experimentally. In fact, we have always found in our experiments that the higher mean flow velocity is, the higher the streaming current. This trend may be explained as follow:

For a laminar flow and for a very long channel, the space charge density convected is constant in terms of the Reynolds number or fluid flow velocity, as could be predicted by the theory. Nevertheless, if the pipe is not long enough, it decreases with the mean velocity or the Reynolds number [43]. In our experimental facility, the channel has a 30 cm in length, whereas, in the numerical simulation, we have reduced this length to 8 cm to reduce the time of calculation. Furthermore, the ratio between time of contact, (between the solid and the liquid), and the EDL development time is an important factor which controls the convected space charge density and consequently the streaming current. So the competitions between this channel length, the mean flow velocity and the reaction rates, which were considered for this simulation, may be responsible for this particular behavior.

9 TIME INTERVAL BETWEEN TWO CONSECUTIVE RUNS

During test, the streaming current's peak value varies depending on the time at which the flow was stopped between two consecutive runs, for a given flow rate. Also, the peak value increases with time to reach a constant value after long time (t→∞) as has been observed experimentally [1, 10, 26].

The streaming current's peak values are calculated at different times, which are corresponding to a partially developed EDL, and compared with those for a fully developed one as shown from Figure 10. This evolution indicates that the streaming current's peak value increases with the time between two consecutive runs to reach a constant value which is corresponding to a fully developed EDL.

10 CONVECTED SPACE CHARGE DENSITY

For a laminar flow and for a very long channel, the diffuse layer at the exit of the channel is fully developed, so the space charge density profile is the same as the one for a diffuse layer

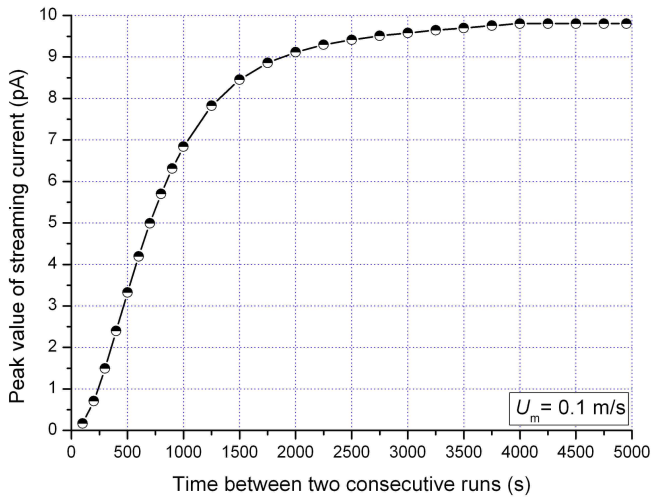

Figure 10. Peak streaming current values (Numerical) as a function of time between two consecutive runs, Mean flow velocity 0.1 m/s.

at rest [43, 44]. Then, the space charge density Q convected by flow, in the channel under test, is given by:

$$Q = \frac{\iint \rho(x,z)\ \ U(x)ds}{\iint U(x)ds} \tag{30}$$

where s is the cross-sectional area of the channel and ρ is the space charge density. The space charge density has to be integrated at the duct's exit to obtain the convected space charge density. Figure 11 shows the evolution of the convected space charge density in terms of liquid conductivity. It is clear that, the space charge density increases in the first part with increase of the liquid conductivity and decrease in the second part and we can explain this trend as follows:

Liquid conductivity varies as well with additive concentrations as with the temperature. In both cases a higher conductivity relates to higher concentrations of positive and negative ions in the liquid. This has two different effects. First, the physicochemical reaction at the interface is reinforced and thus the space charge density on the wall ρ_w is higher as has been shown in Figure 6. Second, the diffuse

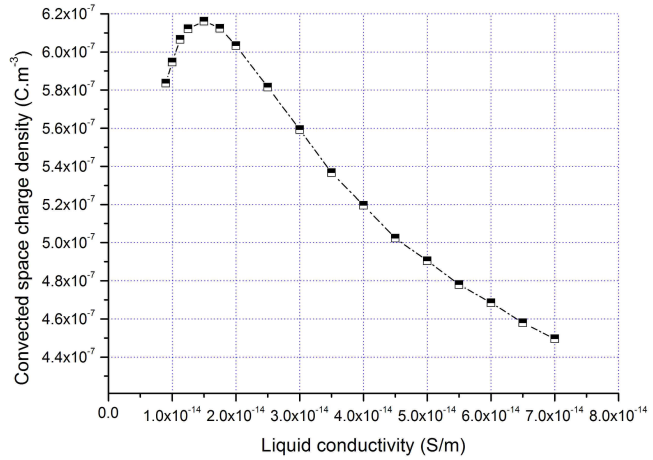

Figure 11. Convected space charge density for different liquid conductivities.

layer thickness δ_0 decreases as it is inversely proportional to the square root of the liquid conductivity. The first effect reinforces the electrification phenomenon, while the second one has an opposite effect as the charge is closer to the wall and thus less convected by the flow. The conjunction of these two opposite effects results generally in the appearance of a maximum of the phenomenon evolution in terms of conductivity or the well-known Van der Minne evolution as shown in Figure 12.

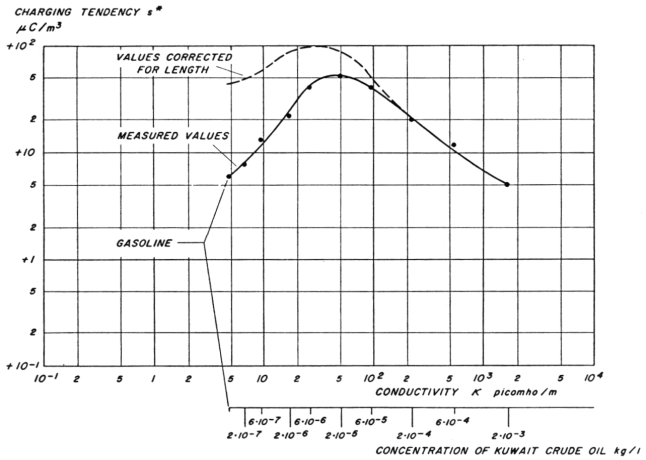

Figure 12. Van der Minne curve: convected space charge density versus gasoline conductivity [9].

11 CONCLUSION

One of the most important parameters which control the Electrical Double Layer (EDL) development is the physicochemical process at the interface between solid and liquid. To date, this process is still under investigation. In an attempt at contributing this investigation, a physicochemical model is proposed in a way analogous to the well known physicochemical corrosion model.

In this paper, we presented a numerical simulation of the EDL development process in the case of a dielectric solid and a liquid containing additives or impurities which are partially dissociated into positive and negative ions. We have considered the case of laminar flow and an interfacial reaction whose conversion is small compared to the concentration of positive and negative ions in the bulk solution. The equations governing this problem are coupled and nonlinear which make the interpretation of the results rather complicated. Nevertheless, some behaviors have been identified and compared with our experimental results and knowledge.

Most of the physical and chemical parameters for this physicochemical EDL development process have not been accessible. Some of the empirical and estimated parameters are proposed to calibrate this numerical model. Irrespective of the slight difference from the order of magnitude point of view, the model was able to correctly simulate the general tendency (dynamics) of the EDL development which agrees with our experimental results and knowledge. Since these parameters are estimated in an arbitrary way, a wider range of data could be qualitatively and quantitatively tested.

To analyze the phenomenon of flow electrification, first it is important to know the space charge density profile for a diffuse layer at rest (static case) in the channel (without any flow), and then we should understand how it is affected by the flow (dynamic case). However, the knowledge of charge distribution in the system was sufficient to visualize the process of charge transport and better understand the behavior of this system.

For the static case: the phenomenon is controlled by diffusion and migration. However, when the liquid is put in contact with the solid, a physicochemical reaction occurs at their interface leading to the formation of EDL. Also, for the present reaction rates and relaxation time for the considered liquid, it seems not applicable to consider neither the instantaneous establishment of space charge profile nor the instantaneous formation of all the space charge at the interface (and then its diffusion). The solution may be found to be between these two asymptotic descriptions.

For the dynamic case: there was encouraging agreement between the experimental and simulated results which enables us to express some general predictions concerning the evolution of the convected space charge density in terms of both flow velocity and concentration of additives. In terms of a laminar flow and for a pipe which is not long enough, the peak value of streaming current increases with the increase in mean flow velocity. In terms of increasing the concentration of additives, the conductivity and the space charge density on the wall increase, but these two parameters act in opposite direction, so the space charge density convected generally passes through a maximum.

However, the insights obtained from the simulation reveal the cause for the evolution of phenomenon in a way that no existing instrumentation could. Furthermore, the simulation also allows one to examine a wide range of parameters in flow; oil characteristics and geometry that would require much more time and expense to investigate experimentally.

ACKNOWLEDGMENT

M. EL-Adawy would like to thank both the staff and technicians in Institut P' UPR 3346. He would also like to thank both the University of Poitiers (France) and Mansoura University (Egypt).

REFERENCES

[1] M. EL-Adawy, J. M. Cabaleiro, T. Paillat, O. Moreau and G. Touchard, "Experimental determination of space charge density associated with flow electrification phenomenon: Application to power transformers", J. Electrostatics, Vol. 67, pp. 354-358, 2009.

[2] G. Touchard, T.W. Patzek and C.J. Radke, "A physicochemical explanation for flow electrification in low-conductivity liquids", IEEE Trans. Industry Applications Vol. 32, pp. 1051-1057, 1996.

[3] I. A. Metwally, "Influence of Solid Insulating Phase on Streaming Electrification of Transformer Oil", IEEE Trans. Dielectr. Electr. Insul, Vol. 4, pp. 327-340, 1997.

[4] H. Wu and S. Jayaram, "dc Field Effects on streaming Electrification in Insulating Oils", IEEE Trans. Dielectr. Electr. Insul, Vol. 3, pp. 499-506, 1996.
[5] T. Paillat, J.M. Cabaleiro, H. Romat and G. Touchard, "Flow electrification process: the physicochemical corroding model revisited", IEEE Int'l. Conf. Dielectr. Liquids (ICDL), pp. 433–436, 2008.
[6] H. Walmsley and G. Woodford, "The generation of electric currents by laminar flow of dielectric liquids", J. Phys. D: Appl. Phys., Vol. 14, pp. 1761–1782, 1981.
[7] J. Gavis and I. Koszman, "Development of charge in low conductivity liquids flowing past surfaces: a theory of the phenomena in tubes", J. Colloid Science, Vol. 16, pp. 375–391, 1961.
[8] T.V. Oommen and S.R. Lindgren, "Streaming electrification study of transformer insulation system using a paper tube model", IEEE Trans. Power Delivery, Vol. 5, pp. 972–983, 1990.
[9] T. Paillat, E. Moreau and G. Touchard, "Space charge density at the wall in the case of heptane flowing through an insulating pipe", J. Electrostatics, Vol. 53, pp. 171–182, 2001.
[10] M. EL-Adawy, T. Paillat, Y. Bertrand, O. Moreau and G. Touchard, "Physicochemical analysis at the interface between conductive solid and dielectric liquid for flow electrification phenomenon", IEEE Trans. Industry Appl., Vol. 46, pp. 1593-1600, July/August 2009.
[11] Y. H. Paik, W. J. Yoon and H. C. Shin, "Static electrification of solid oxide in liquid metal and electrical double layer at the interface", J. Colloid and Interface Sci., Vol. 269, pp. 354-357, 2004.
[12] D. Pierre, J. C. Viala, M. Peronnet, F. Bosselet and J. Bouix, "Interface reactions between mild steel and liquid Mg-Mn alloys", Materials Sci. Engineering, Vol. A349, pp. 256-264, 2003.
[13] J. E. Castle and H. G. Masterson, "The role of diffusion in the oxidation of mild steel in high temperature aqueous solutions", J. Corrosion Science, Vol. 6, pp. 93-104, 1966.
[14] L. Martinelli, F. Balbaud-Céléier, G. Picard and G. Santarini, "Oxidation mechanism of a Fe-9Cr-1 Mo steel by liquid Pb-Bi eutectic alloy (Part III)", J. Corrosion Sci., Vol. 50, pp. 2549-2559, 2008.
[15] A. P. Washabaugh and M. Zahn, "A Chemical Reaction-Based Boundary Condition For Flow Electrification", IEEE Trans. Dielectr. Electr. Insul, Vol. 4, pp. 688–709, 1997.
[16] J. R. Melcher, *Continuum Electromechanics*, M.I.T. Press, Cambridge, Mass., USA, 1981.
[17] Equipe de développement de Code_Saturne, "Documentation théorique et informatique du noyau de Code_Saturne version 1.2", EDF R&D, 2006.
[18] M. Sakiz and F. Archambeau, "Guide pratique d'utilisation de Code_Saturne version 1.2", EDF R&D, 2005.
[19] F. Archambeau, N. Méchitoua and M. Sakiz, "Code_Saturne: a Finite Volume Code for the Computation of Turbulent Incompressible Flows", Industrial Applications, Int'l. J. Finite Volumes, Vol. 1, pp. 1-62, 2004.
[20] R. Tobazéon, "Conduction électrique dans les liquides", Techniques de l'Ingénieur, Paris, France, D 2 430, 2006.
[21] J. M. Cabaleiro, *Etude du développement de la double couche électrique lors de la mise en écoulement d'un liquide diélectrique dans une conduite isolante*, Ph.D. thesis, LEA of Poitiers, France, 2007.
[22] R. B. Bird, W. E. Stewart and E. N. Lightfoot, *Transport Phenomena*, John Wiley & Sons, New York, NY, USA, 1960.
[23] G. Touchard, H. Romat, P. O. Grimaud and S. Watanabe, "Solution for the electrical interfacial problem between a dielectric liquid and a metallic wall", IEEE 4th Int'l. Conf. Properties and Application of Dielectric Materials, pp. 336-339, 1994.
[24] O. Moreau, T. Paillat and G. Touchard, "Flow Electrification in Transformers: Sensor Prototype for Electrostatic Hazard", Inst. Physics Conf. Series, UK, Vol. 178, pp. 31-36, 2003.
[25] J. Martin Cabaleiro, T. Paillat, O. Moreau and G. Touchard, "Electrical Double layer's Development Analysis: Application to Flow Electrification in Power Transformers", IEEE Trans. Industry Appl. Vol. 45, pp. 597-605, 2009.
[26] J. M. Cabaleiro, T. Paillat, O. Moreau and G. Touchard, "Flow electrification of dielectric liquids in insulting channels: Limits to the application of the classical wall current expression", J. Electrostatics, Vol. 66, pp. 79-83, 2008.
[27] J. A. Palmer and J. K. Nelson, "The simulation of short-term streaming electrification dynamics", J. Phys. D: Appl. Phys, Vol. 30, pp. 1207-1213, 1997.
[28] T. Paillat, E. Moreau and G. Touchard, "Streaming electrification of a dielectric liquid through a glass capillary", IEEE Industry Applications Conf., Vol. 2, pp. 743–748, 2000.
[29] A. Bourgeois, *Etude du phenomena d'électristaion par écoulement sur les cartons des transformateur de puissance*, Ph.D. dissertation, INP de Grenoble, Grenoble, France, 2007.
[30] A. Bourgeois, T. Paillat, O. Moreau, G. Mortha and G. Touchard, "Flow electrification in power transformers: salt-type additive as a potential remedy", J. Electrostatics, Vol. 63, pp. 877-882, 2005.
[31] A. Bourgeois, G. Mortha, T. Paillat, G. Touchard, O. Moreau and Y. Bertrand, "Flow electrification in power transformer: Study of a potential remedy", IEEE Trans. Dielectr. Electr. Insul, Vol. 13, pp. 650-656, 2006.
[32] G. Touchard, "Flow Electrification," J. Electrostatics, Vol. 51-52, pp. 440-447, 2001.
[33] J. M. Cabaleiro, T. Paillat, O. Moreau and G. Touchard, "Parametric Study by Electrical Analogy: Application to Flow Electrification in Power Transformers", Proc. Electrostatic Society of America/ Institute of Electrostatics Japan/ IEEE-Industry Applications Society/ Société Française d'Electrostatique Joint Conf. Electrostatics, pp. 458469, 2006.
[34] T. Paillat, O. Moreau, J. M. Cabaleiro, F. Perisse and G. Touchard, "Electrisation par écoulement: Modélisation électrique", J. Electrostatics, Vol. 64, pp. 485-491, 2006.
[35] O. Moreau and Gérard Touchard, "Experimental Study and Modeling of Static Electrification in Power Transformers", IEEE Trans Industry Application, Vol. 37, pp. 971-977, 2001.
[36] A. P. Washabaugh and M. Zahn, "Flow Electrification Measurements of Transformer Insulation using a Couette Flow Facility", IEEE Trans. Dielectr. Electr. Insul, Vol. 3, pp. 161-187, 1996.
[37] H. Chen, G. G. Touchard and C. J. Radke, "A Linearized Corrosion Double-Layer Model for Laminar Flow Electrification of Hydrocarbon Liquids in Metal Pipes", Ind. Eng. Chem. Res., Vol. 35, pp. 3195-3202, 1996.
[38] P. Fung , H. Chert , G. G. Touchard and C. J. Radke, "A Nonlinear Corrosion Double-Layer Model for Laminar Flow Electrification of Hydrocarbon Liquids in Long Metal Pipes", J. Electrostatics, Vol. 40-41, pp. 45-53, 1997.
[39] H. Miyao, M. Higaki and Y. Kamata, "Influence of AC and DC Fields on Streaming Electrification of Transformer Oil", IEEE Trans. Electr. Insul, Vol. 23, pp. 129-135, 1988.
[40] T. J. Harvey, R. J. K. Wood, G. Denuault and H. E. G. Powrie, "Effect of oil quality on electrostatic charge generation and transport", J. Electrostatics, Vol. 55, pp. 1-23, 2002.
[41] J. K. Nelson, "Dielectric Fluids in Motion", IEEE Electr. Insul. Mag., Vol. 10, No. 3, pp.16-28, 1994.
[42] G. Touchard, M. Benyamina, J.A. G. Borzeix and H. Romat, "Static Electrification by Laminar Flow Through Artificially Roughed Pipes", IEEE Trans. Industry Appl., Vol. 25, pp.1067-1072, November/December 1989.
[43] G. Touchard, "Flow Electrification of Liquids," J.-S. Chang, A. J. Kelly and J. M. Crowley, Editors, *Handbook of Electrostatic Processes*, Marcel Dekker, New York, pp. 83–87, Chapter 5, 1995.
[44] E. Moreau, T. Paillat and G. Touchard, "Flow Electrification in High Power Transformers: BTA Effect of Pressboard Degraded by Electrical Discharges", IEEE Trans. Dielectr. Electr. Insul, Vol. 10, pp. 15-21, 2003.

Mohamed EL-Adawy was born in Egypt in 1975. He received the B.Eng. degree in electrical engineering and the M.Eng. degree in high-voltage engineering from Mansoura University, Mansoura, Egypt, in 1997 and 2003, respectively. He received the Ph.D. degree from the Institut P' UPR 3346, the Electro-Fluid Dynamics Group, , Centre National de la Recherche Scientifique, University of Poitiers, Poitiers, France, in 2011. His areas of research include oil-flow electrification in electric power apparatus, fundamental aspects of the electrical double layer and its modeling, power system overvoltage, generation and measurement of impulse voltage, characterization of impulse voltage and modeling of power transformers.

Thierry Paillat was born in Parthenay, France, in 1971. He received the B.S. degree in physics and electrical engineering and the Ph.D. degree from the University of Poitiers, Poitiers, France, in 1998. Since 1998, he has been an Assistant Professor with the Electrokinetic Team, Institut P' UPR 3346, Centre National de la Recherche Scientifique, University of Poitiers. His research focuses on electrostatic hazards by flow electrification of fluids and fundamental aspects of an electric double layer.

Juan Martin Cabaleiro was born in 1978. He graduated in mechanical engineering at the University of Buenos Aires in 2004, and received the Ph.D. degree from the University of Poitiers, in Poitiers, France in 2007. He is a researcher at the Fluid Dynamics Laboratory, at the Faculty of engineering of the University of Buenos Aires, and at the Microfluidics laboratory of the University of the Mercantile Marine, in Buenos Aires. His research interests include electrostatic hazards by flow electrification, fundamental aspects of the electrical double layer and liquids' flow control by EHD actuators in microchannels and microjets.

Gérard Touchard was born in France in 1944. He received the "Doctor és Sciences Physiques" degree from the University of Poitiers, Poitiers, France, in 1978. In 1977, he established the Electro-Fluid Dynamics Group, Institut P' UPR 3346, Centre National de la Recherche Scientifique, University of Poitiers, where he has remained Head for 30 years. He became a Full Professor in 1987. During 1980–1981, he was a Visiting Researcher at the Massachusetts Institute of Technology, Cambridge. During 1993–1994, he was a Visiting Researcher at the University of California, Berkeley. He is the author or coauthor of more than 350 papers. His research interests focus on interactions between flows and electrical phenomena. Dr. Touchard is a member of the Russian Academy of Engineering. He established the Société Française d'Electrostatique in 1997 and remains its Chairman. He has organized several international conferences on electrostatics. Professor Touchard is an Associate Editor of the IEEE Transactions on Dielectrics and Electrical Insulation Society.